AD-A284 072

EDGEWOOD

RESEARCH, DEVELOPMENT & ENGINEERING CENTER

U.S. ARMY CHEMICAL AND BIOLOGICAL DEFENSE COMMAND

ERDEC-TR-168

SCREENING SMOKE PERFORMANCE OF COMMERCIALLY AVAILABLE POWDERS

II. VISIBLE SCREENING BY TITANIUM DIOXIDE

Janon F. Embury
Donald Walker

RESEARCH AND TECHNOLOGY DIRECTORATE

Curtis J. Zimmermann

GEO-CENTERS, INCORPORATED
Fort Washington, MD 20744

June 1994

CUM SCIENTIA DEFENDIMUS

Aberdeen Proving Ground, MD 21010-5423

Disclaimer

The findings in this report are not to be construed as an official Department of the Army position unless so designated by other authorizing documents.

REPORT DOCUMENTATION PAGE

Form Approved
OMB No 0704-0188

1. AGENCY USE ONLY (Leave blank)	2. REPORT DATE	3. REPORT TYPE AND DATES COVERED
	1994 June	Final, 91 Aug - 93 Feb

4. TITLE AND SUBTITLE
Screening Smoke Performance of Commercially Available Powders
II. Visible Screening by Titanium Dioxide

5. FUNDING NUMBERS
PR-10464609D200

6. AUTHOR(S)
Embury, Janon F.; Walker, Donald (ERDEC); and Zimmermann, Curtis J. (GEO-CENTERS, INC.)*

7. PERFORMING ORGANIZATION NAME(S) AND ADDRESS(ES)
DIR, ERDEC,** ATTN: SCBRD-RTB, APG, MD 21010-5423

GEO-CENTERS, INC., Fort Washington, MD 20744

8. PERFORMING ORGANIZATION REPORT NUMBER
ERDEC-TR-168

9. SPONSORING/MONITORING AGENCY NAME(S) AND ADDRESS(ES)

10. SPONSORING/MONITORING AGENCY REPORT NUMBER

11. SUPPLEMENTARY NOTES
*Curtis Zimmermann is currently employed by the Mearl Corporation, Ossining, NY 10562 (Continued on page ii)

12a. DISTRIBUTION/AVAILABILITY STATEMENT
Approved for public release; distribution is unlimited.

12b. DISTRIBUTION CODE

13. ABSTRACT *(Maximum 200 words)*

The visible and infrared smoke screening performance of a variety of commercially available titanium dioxide pigments have been evaluated in the ERDEC 14 m^3 smoke chamber. Four performance parameters-extinction coefficient, dissemination yield, particle density and deposition velocity have been identified and measured to predict screening performance in the field. Weight, volume and cost constrained figures of merit based on these performance parameters have been measured and tabulated for the visible, mid IR and for IR bands as well as 1.06 μm wavelength in order to rate their relative screening capabilities.

14. SUBJECT TERMS
Titanium dioxide
Aerosol deposition
Aerosol coagulation
Electrostatic aerosol dispersion
Visible screening

15. NUMBER OF PAGES
28

16. PRICE CODE

17. SECURITY CLASSIFICATION OF REPORT	18. SECURITY CLASSIFICATION OF THIS PAGE	19. SECURITY CLASSIFICATION OF ABSTRACT	20. LIMITATION OF ABSTRACT
UNCLASSIFIED	UNCLASSIFIED	UNCLASSIFIED	UL

11. SUPPLEMENTARY NOTES (Continued)

**When this study was conducted, ERDEC was known as the U.S. Army Chemical Research, Development and Engineering Center, and the ERDEC authors were assigned to the Research Directorate.

PREFACE

The work described in this report was authorized under Project No. 10464609D200, Screening Smoke Materiel Engineering. This work was started in August 1991 and completed in February 1993.

The use of trade names or manufacturers' names in this report does not constitute an official endorsement of any commercial products. This report may not be cited for purposes of advertisement.

This report has been approved for release to the public. Registered users should request additional copies from the Defense Technical Information Center; unregistered users should direct such requests to the National Technical Information Service.

Blank

TABLE OF CONTENTS

LIST OF FIGURES

LIST OF TABLES

Blank

SCREENING SMOKE PERFORMANCE OF COMMERCIALLY AVAILABLE POWDERS

II. VISIBLE SCREENING BY TITANIUM DIOXIDE

INTRODUCTION

Titanium dioxide (titania, TiO_2) is a material that has been carefully engineered both chemically and physically to be very efficient at scattering light so that when incorporated into a paint for example, a minimum number of coats will hide a substrate. For a unique application such as military visible obscuration, control over the physical and chemical properties of the pigment is also of great importance. Historically manufacturers have maximized the extinction coefficient (α), electromagnetic extinction cross section per mass of material, for the pigment industry by adjusting pigment particle diameter until maximum substrate hiding power was achieved resulting in an optimum diameter approximately equal to 0.25 microns for the rutile form of TiO_2 having a refractive index of 2.73. The anatase form of TiO_2 has a slightly lower refractive index (2.55) and therefore a slightly larger optimized diameter and a slightly lower extinction cross section per volume.

Titania is an efficient scatterer of light compared to other materials because of its relatively large refractive index. Because maximum achievable electromagnetic cross section per volume of scattering material, extinction coefficient multiplied by density ($\alpha * \rho$), is roughly inversely proportional to optimum diameter, and since optimum diameter decreases with increasing refractive index, we find that titanium dioxide pigment has a volume limited figure of merit $\Phi_V = \alpha * Y * \rho$ superior to other lower refractive index white pigments such as antimony oxide with a refractive index in the range 2.09-2.29 and zinc oxide with a refractive index of 2.02. The performance parameters α, yield Y and density ρ along with the weight Φ_W, volume Φ_V and financial Φ_F limited figures of merit for numerous grades of commercially available titania are listed in Table 1. Performance parameters and figures of merit (FOM), as described in the first report in this series that surveyed sources of graphite flake powder for infrared screening, allow for complete performance characterization and comparison among obscurant materials[1].

Titania has a volume limited figure of merit ($\Phi_V = \alpha * Y * \rho$) about three times greater than fog oil and comparable to white phosphorus (WP). White phosphorus has a low humidity yield factor $Y = 3$, about three times greater than that achievable by any powder such as titania because WP reacts with the air adding aerosol mass by condensing water vapor and consuming oxygen. On the other hand titania has a value for $\alpha * \rho$ that is almost three times that of WP or fog oil. Figure 1 shows photopic average electromagnetic cross section per volume $\alpha * \rho$ as a function of mass median diameter for log normal polydispersions with geometric standard deviations of 1.4. Each curve corresponds to a different refractive index N. The lowest broadest curve peaks at the largest mass median diameter of about 3/4 micron and corresponds to a refractive index of 1.4 typical of fog oil and WP, while the middle curve corresponds to a refractive index of 2.0 and the curve with the highest and most narrow peak reaching its peak value at the smallest mass median diameter, about 1/5 micron, corresponds to a refractive index of 3. The extinction coefficient was computed by averaging over both aerosol size distribution and over visible wavelengths using the photopic response of the eye as a weighting function.

The goal of smoke screening material development is to maximize the product of smoke plume optical depth multiplied by operational lifetime (duration) for a given volume of material transported. When transportation is volume limited, optical depth multiplied by duration is proportional to $\alpha * Y * \rho$ multiplied by the fraction of initial aerosol mass remaining airborne downwind ($\alpha Y \rho e^{-\gamma v_D}$) where the coefficient "γ" depends on Pasquill category, windspeed and distance downwind[1]. Thus the optical depth multiplied by the duration can be maximized by maximizing $\alpha Y \rho e^{-\gamma v_D}$, a figure of merit based on the three performance parameters alpha α, yield Y and deposition velocity v_D that can be easily measured in an aerosol chamber, but not in the field. The density referred to above is that of the packed powder being transported. Its upper limit is the intrinsic particle density and because of variability in packing processes that densify powders we use this upper limit as the fourth performance parameter appearing in Table 1. When transport is weight limited, optical depth multiplied by duration is proportional to a second figure of merit $\alpha Y e^{-\gamma v_D}$. Close to the source these figures of merit to be maximized become simply $\alpha Y \rho$ and αY for volume and weight limited transport respectively. In other words we want to maximize the square meters of screening cross section per volume of transported aerosolized material when volume limited or square meters of screening per mass of transported aerosolized material when weight limited.

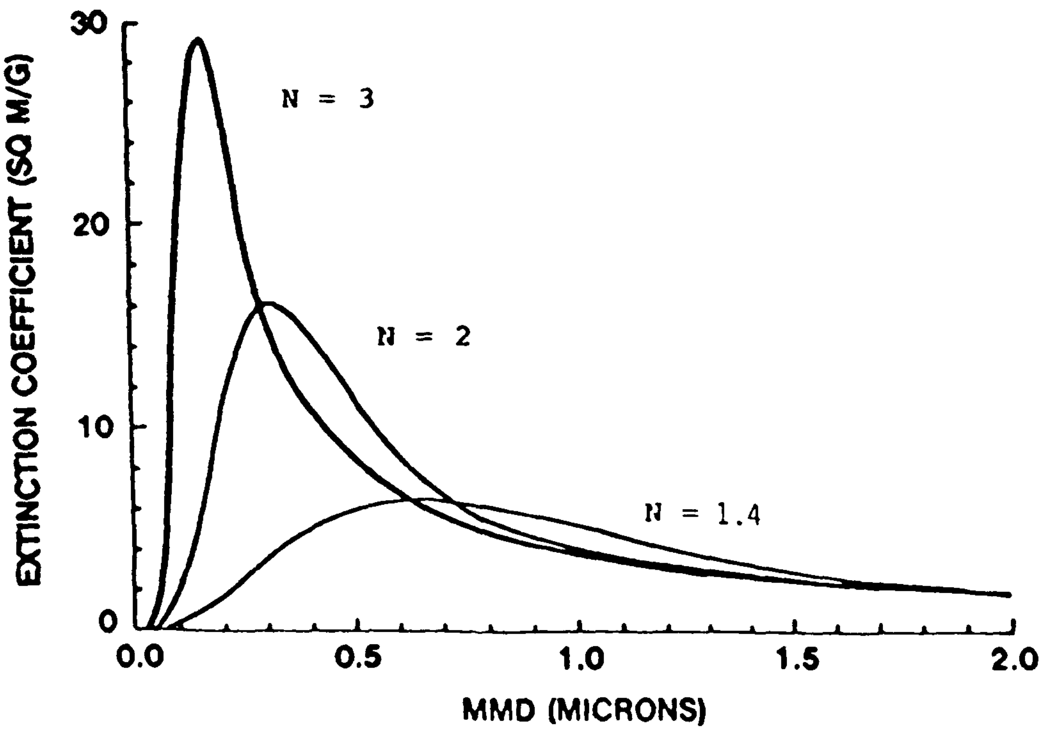

Figure 1.[2] Photopic average electromagnetic cross section per volume $\alpha * \rho$ as a function of mass median diameter for log normal polydispersions with a geometric standard deviation of 1.4.

AEROSOL DEPOSITION

The rate of which aerosol particles are removed from the air and deposited onto the terrain depends upon four mechanisms: gravitational settling, impaction, Brownian diffusion and turbulent diffusion (this can also lead to reaerosolization). The dominant mechanism for submicron particles is Brownian diffusion while the dominant mechanism for large particles over 10 microns aerodynamic diameter is gravitational settling. The net effect of deposition can be studied in the ERDEC smoke chamber (Figure 2) by stirring the aerosol not only to maintain uniform aerosol concentration, but also to create a level of air turbulence that will produce an aerosol deposition velocity representative of what could be expected in the field under typical meteorological and terrain conditions. The stirred settling model[3] for a rectangular chamber of height H, floor area A and volume $V = AH$, requires that concentration C be maintained uniform throughout so that we can relate an aerosol deposition velocity v_D to a rate of change dm/dt of total aerosol mass m contained in the chamber as a function of time t

$$\frac{dm}{dt} = -v_D A C$$

Expressing total aerosol mass $m = CV$ in terms of concentration this becomes

$$\frac{d(CV)}{dt} = -v_D A C$$

The aerosol test chamber volume is constant so we write

$$\frac{dC}{C} = \frac{-v_D A}{V} dt = -v_D \frac{dt}{H}$$

which has the solution

$$C = C_0 e^{\frac{-v_D t}{H}}$$

If deposition is dominated by gravitational settling we can approximate deposition velocity using the Stokes settling velocity. Deposition velocities of the various titania materials have been measured in the smoke chamber with an average value of roughly 0.03 cm/sec. There are a wide range of values for the deposition velocity depending upon the material tested but this is probably in part due to the relatively small differences in aerosol concentrations measured on sequential filter samples leading to small computed deposition velocities and large percentage errors.

Variability in measured deposition velocity is the result of errors in several measured quantities which are then used to compute deposition velocity. We compute deposition velocity v_D using the stirred settling model and two filter sample concentration measurements, c_1, and c_2, of one minute duration commencing at times t_1 and t_2

$$v_D = \frac{H}{t_2 - t_1} \ln\left(\frac{c_1}{c_2}\right)$$

Thus measurement errors in chamber height δH, time δt and concentration δc result in the following root mean square (rms) error in deposition velocity

$$\langle \delta v_D \rangle = \sqrt{\left(\frac{\partial v_D}{\partial H}\delta H\right)^2 + \left(\frac{\partial v_D}{\partial t_1}\delta t_1\right)^2 + \left(\frac{\partial v_D}{\partial t_2}\delta t_2\right)^2 + \left(\frac{\partial v_D}{\partial c_1}\delta c_1\right)^2 + \left(\frac{\partial v_D}{\partial c_2}\delta c_2\right)^2}$$

When comparing values of $\langle \delta v_D \rangle$ based on measurements in the ERDEC 14 cubic meter smoke chamber we can drop the first error term since chamber height has been measured just once and that value is used in all computations of deposition velocity. The error terms involving concentration must be farther broken down since concentration is actually computed as a function of a time duration measurement τ, air volumetric flow rate measurement $\dot{V}$ using a rotometer and two mass measurements, filter tare m_t and filter plus aerosol material m_T.

$$c = \frac{m_T - m_t}{\dot{V}\tau}$$

and

$$\langle \delta c \rangle = \sqrt{\left(\frac{\partial c}{\partial \tau}\delta \tau\right)^2 + \left(\frac{\partial c}{\partial \dot{V}}\delta \dot{V}\right)^2 + \left(\frac{\partial c}{\partial m_t}\delta m_t\right)^2 + \left(\frac{\partial c}{\partial m_T}\delta m_T\right)^2}$$

Solving for the partial derivatives

$$\frac{\partial v_D}{\partial t} = \frac{v_D}{t_2 - t_1}$$

$$\frac{\partial v_D}{\partial c} = \frac{H}{c(t_2 - t_1)}$$

$$\frac{\partial c}{\partial \tau} = \frac{c}{\tau}$$

$$\frac{\partial c}{\partial \dot{V}} = \frac{c}{\dot{V}}$$

$$\frac{\partial c}{\partial m} = \frac{c}{m_T - m_t}$$

The rms error in deposition velocity when $\delta t = \delta t_1 = \delta t_2 = \delta \tau$ and when $\delta m = \delta m_t = \delta m_T$ becomes

$$\langle \delta v_D \rangle = \sqrt{2\, v_D^2\left(\frac{\delta t}{t_2 - t_1}\right)^2 + 2\left(\frac{H}{t_2 - t_1}\right)^2\left[\left(\frac{\delta t}{\tau}\right)^2 + \left(\frac{\delta \dot{V}}{\dot{V}}\right)^2 + 2\left(\frac{\delta m}{m_T - m_t}\right)^2\right]}$$

The chamber height is 200cm, the time interval between start times for sequential filter samples is t_2-t_1=150s, the duration of each filter sample is τ=60s, the time measurement error is δt=0.5s, the 20 lpm flow rate error is $\frac{\delta \dot{V}}{\dot{V}} \approx 0.02$, the aerosol mass deposited on the filter at a typical concentration of 0.2g/m^3 is m_T-$m_t \approx$0.044g, the weighting error is 0.00002g and a deposition velocity typical of TiO_2 is $v_D = 0.03 cm/s$. The expected rms error in deposition velocity is therefore

$$\langle \delta v_D \rangle = \sqrt{2(0.05)^2(\frac{0.5}{150})^2 + 2(\frac{200}{150})^2[(\frac{0.5}{60})^2 + (0.02)^2 + 2(\frac{0.00002}{0.004})^2]}$$

$$= \sqrt{5.6X10^{-8} + 3.6[6.9X10^{-5} + 4X10^{-4} + 5X10^{-5}]}$$

So the first term, the one dependent upon the deposition velocity is small compared to the remaining three error terms which combine to give a rms error of

$$\langle \delta v_D \rangle = 0.043 \text{cm / sec}$$

which is comparable to measured deposition velocities for TiO_2. This explains the large observed variability in the tabulated deposition velocities measured in the chamber. It should be mentioned that the deposition velocity is influenced by the level of turbulence generated by the mixing fan. Variability in mixing fan speed has not been addressed in the above error analysis.

To determine whether Brownian diffusion is the dominant deposition mechanism, first we ignore the flux deposited onto the chamber walls and ceiling because deposition is observed to be negligible and must therefore be balanced by reaerosolization. The flux of particles deposited onto the floor due to Brownian diffusion J (particles/cm^{2}sec) alone may be written[3]

$$J = \frac{DC_N}{\Delta}$$

where C_N is the chamber aerosol number concentration, Δ is the laminar flow boundary layer thickness where Brownian diffusive transport becomes more important than turbulant diffusion transport and D is the Brownian diffusion coefficient. We can then write

$$D = B\kappa T = \frac{C_c}{3\pi\eta d}\kappa T$$

where B is the particle mobility, κ is Boltzmann's constant, T is temperature, η is air viscosity, d is particle diameter and C_C is the Cunningham slip correction factor to be defined later. The number flux per unit area per unit time J may be written in terms of aerosol deposition velocity

$$J = v_D C_N$$

thus

$$v_D = \frac{D}{\Delta}$$

Since we measure v_D and can calculate D, we estimate the laminar boundary layer thickness for our level of turbulance

$$\Delta = \frac{D}{v_D} = \frac{C_C \kappa T}{3\pi\eta d v_D}$$

Plugging in some numbers for titania where $d \approx 0.25\mu m$ and $C_C = 1.74$ is derived later

$$\Delta = \frac{(1.74)(1.38X10^{-16})(293)}{(3\pi)(1.83X10^{-4})(0.25X10^{-4})(0.03)} \approx 5X10^{-5}\text{cm}$$

This value is equal to that mentioned earlier by Fuchs[3] for half micron diameter particles and it appears that Brownian diffusion is not the dominant deposition mechanism, but is accompanied by gravitational sedimentation and turbulent diffusion which reduces Δ below the thickness of the laminar sublayer.[5] Inertial impaction driven by turbulent diffusion that brings the particles within a stop distance and gravitational settling will reduce the computed boundary layer thickness to artificially small values for particle diameters greater than a few hundredths of a micron.

AEROSOL COAGULATION

Primary particles of titanium dioxide are roughly isometric spherical particles with a volume equivalent diameter around 1/4 μm and a geometric cross section equivalent diameter around 0.31 μm as found with computed spectra that matches the measurement. At mass concentrations $C_m \approx 0.1$ g/m^3, we have number concentrations of titanium dioxide particles having density $\rho \approx 4$g/cm^3 and diameter $d \approx 0.25$ microns

$$C_N(t=0) = \frac{C_n}{\rho \frac{\pi}{6} d^3} = \frac{(0.1 g/m^3)(10^{-6} m^3/cm^3)}{(4g/cm^3)(\frac{\pi}{6})(0.25X10^{-4}cm)^3} \approx 3X10^6 / \text{cm}^3$$

The Cunningham slip correction factor for these particles is[4]

$$C_C = 1 + \frac{2\lambda}{d}[1.257 + 0.40e^{\frac{-1.1d}{2\lambda}}]$$

where $\lambda \approx 0.07\mu m$ is the mean free path of air molecules at standard temperature and pressure. For $d = 0.25\mu m$ we have $C_C \approx 1.74$ and the coagulation coefficient[4]

$$\text{K} = \frac{8}{3}\frac{\kappa T}{\eta}C_C$$

where η is the viscosity of air, T the temperature and κ the Boltzman constant, becomes

$$\text{K} = \frac{8}{3}\frac{(1.38X10^{-16})(293)}{1.38X10^{-4}}(1.74) = 1.03X10^{-9}\text{cm}^3/\sec$$

The number concentration $C_N(t)$ as a function of time is found to be[4]

$$C_N(t) = \frac{C_N(t=0)}{1 + C_N(t=0)\frac{\text{K}t}{2}}$$

by solving the monodisperse aerosol coagulation equation assuming constant coagulation coefficient. The time required to reduce the concentration to half it's initial value as a result of coagulation is

$$t_{1/2} = \frac{2}{C_N(t=0)\text{K}} = \frac{2}{(3X10^6/cm^3)(1.03X10^{-9}cm^3/\sec)} \approx 670\text{sec}$$

Concentrations are higher near the dissemination source and concentrations during testing are often three times this value thereby reducing the coagulation half life. As a result coagulation does occur during the several minutes of chamber testing and can be observed in aerosol samples studied under the electron microscope. Linear and dendritic chains of primary particles form; some with many branches.

DECREASED YIELD DUE TO ELECTROSTATIC DISPERSION

Unlike graphite powders which experience increases in dissemination yield when dried in an oven, titanium dioxide powders experience a significant reduction in dissemination yield. This is probably the result of triboelectric monopolar charging of the particles as they pass through and collide with the walls of the aluminum feed tube of the dissemination nozzle which is grounded. The charging effect could be virtually eliminated by either breaking the ground or by coating the inside walls of the feed tube with the same material constituting the aerosol. The magnitude of the charge effect on aerosol concentration and yield can be estimated from the expression for the concentration decay of a uniform cloud of identically charged aerosol particles[5]

$$C_N(t) = \frac{C_N(t=0)}{4\pi C_Q \zeta t + 1}$$

where $C_N(t)$ is the aerosol number concentration at time t, C_Q is the initial charge per unit volume of aerosol laden air and ζ is the electrical mobility of the particle. The electrical mobility, defined as the particle velocity divided by the electric field strength E producing that velocity, $\zeta = v / E$, is found by writing the electric force acting on a particle having n elementary charges

$$F_E = nqE$$

and equating it with the drag force acting on the particle

$$F_D = 3\pi\eta d C_C$$

where η is the viscosity of air, d the particle diameter and C_C the Cunningham correction factor. Solving for the velocity and rewriting the expression for mobility

$$\zeta = \frac{ne}{3\pi\eta d C_C}$$

and writing the initial charge concentration in terms of the aerosol particle number concentration and the number of charges per particle

$$C_Q = C_N ne$$

we then substitute these expressions for C_Q and ζ into the expressions describing the decrease in aerosol concentration as the monopolar uniformly charged cloud expands into free space or is intercepted by boundaries such as chamber walls and floor

$$C_N(t) = \frac{C_N(t=0)}{\dfrac{4C_N(t=0)n^2e^2t}{3\eta d C_C} + 1}$$

The time required to reduce the number concentration by half due to monopolar charged cloud expansion is

$$t_{\frac{1}{2}} = \frac{3\eta d C_C}{4C_N(t=0)n^2e^2}$$

Aerosol concentration is measured and averaged over the period of one minute commencing immediately after aerosol dissemination to obtain dissemination yield of the powder. We roughly estimate the concentration half life due to charged cloud expansion at half a minute since subsequent concentration decay, as indicated by the second and third filter samples, appears to be that expected due to a combination of gravitational settling plus inertial impaction driven by turbulence. We use the initial number concentration of $3X10^6$ and solve for ne, the charge on each particle in esu using the cgs system,

$$ne = \sqrt{\frac{3\eta dC}{4C_N(t=0)t_{\frac{1}{2}}}}$$

$$ne = \sqrt{\frac{3(1.83X10^{-4})(0.25X10^{-4})(1.74)}{4(3.0X10^{6})30}} = 8X10^{-9}\text{esu}$$

The fundamental unit of charge is $e=4.8X10^{-10}$ esu. We solve for the average number of fundamental charges per particle and obtain

$$n = \frac{8X10^{-9}esu}{4.8X10^{-10}esu} = 16.7\text{charges / particle}$$

The number is not terribly sensitive to the half life we have estimated; proportional to the inverse square root. Had we choosen a half life of 3 seconds instead of 30 seconds the number would become 52.8 charges/particle. We can estimate the current flowing through the inner feed tube of the dissemination nozzle by noting that $e=1.6X10^{-19}$ coulombs in the mks system of nomenclature. Assuming that the material is disseminated into the chamber volume V during the time t_D, we can expect a total aerosol charge Q results in a current I equal to

$$I = \frac{Q}{t_D} = \frac{VC_N(t=0)ne}{t_D}$$

$$I \approx \frac{14(3X10^{12})(16.7)(1.6X10^{-19})}{10} \approx 11.2\mu\text{amps}$$

a quantity that can be measured.

It should be emphasized that some of these computations involve simplifying assumptions that guarantee no better than perhaps order of magnitude accuracy. Nevertheless the calculations are essential not only to understand dominant effects and phenomena but are invaluable in guiding experimentation by providing an understanding of how measured quantities depend on independent variables.

TITANIUM DIOXIDE MANUFACTURING

Currently titania (both rutile and anatase crystal forms) is the most important commercially produced white pigment throughout the world, with rutile grades being produced in greatest volume. The pigment is extensively used because it efficiently scatters visible light thereby giving whiteness, brightness and opacity when incorporated into a paint, plastic or paper product.

There are two manufacturing processes used for production of titanium dioxide known as the sulfate and chloride processes. The older sulfate process, originally only producing anatase grades but later developed to produce rutile grades, typically involves the reaction of titanium bearing ore with sulfuric acid at elevated temperatures to produce a solution of titanium, iron and other metal sulfates. The sulfate solution undergoes a number of processes to allow for extraction of the purified titanyl sulfate, which then proceeds through a series of steps including hydrolysis, precipitation, washing and calcination to produce pigmentary titania. The desired anatase or rutile crystal structure and size is controlled by nucleation and calcination of the pigment. The more modern chloride process (commercialized by Du Pont to produce rutile titania) involves the formation of titanium tetrachloride from high purity titanium bearing ore reacting with chlorine gas in the presence of coke. The tetrachloride is then further purified by distillation and then oxidized at high temperature the vapor phase to produce crystalline titanium dioxide. Crystal type anc icle size distribution can be controlled by the oxidation step. Both crystalline forms of the oxide, regardless of the manufacturing route, routinely have surface treatments applied to the base pigment. Typically a hydrous oxide of alumina, silica or zirconia is applied to the surface to improve anti-yellowing, dispersibility and durability. Individual oxide treatment or various mixed combinations can be used to taylor surface acidity and/or charge in an effort to optimize performance depending on the specific application. Some grades of titania are further treated after the oxide coating with organics such as polyols, amines and siloxanes. These coatings can be used to obtain hydrophobic/hydrophilic behavior at the surface of the base pigment and also impart improved powder flow/dispersion properties.[6]

ERDEC SMOKE CHAMBER

The 14 cubic meter smoke chamber used to measure the performance parameters such as the electromagnetic extinction cross section per mass of aerosol (α), yield (Y) and deposition velocity (v_D) is shown in Figure 2 with the full smoke characterization instrument configuration. Glass fiber filters, a rotometer and vacuum pump are used to measure aerosol concentration at a flow rate of 20 liters per minute. A photodiode array spectrometer measures aerosol transmittance over the wavelength range of 0.4μ-1.0μ. Two FTIR spectrometers measure aerosol transmittance over the spectral regions 0.9μ-3μ and 2.5μ-22μ. At reduced concentrations a quartz crystal microbalance (QCM) and an aerodynamic particle sizer (APS) measure aerodynamic particle size distribution. The Stanford Research Institute sonic pneumatic nozzle is operated at 60 psi to disperse and deaggregate powders to produce an aerosol of primary particles.[7] A mixing fan is operated continuously in the chamber at a low speed to maintain uniform concentration and provide a level of turbulence driving reaerosolization and impaction approximating those components of aerosol deposition in the battlefield. The aerosol sedimentation component of deposition will of course be independent of whether the aerosol is in a chamber or on the battlefield. All titanium dioxide samples tested were previously oven dried and cooled in a desiccator prior to aerosol dissemination.

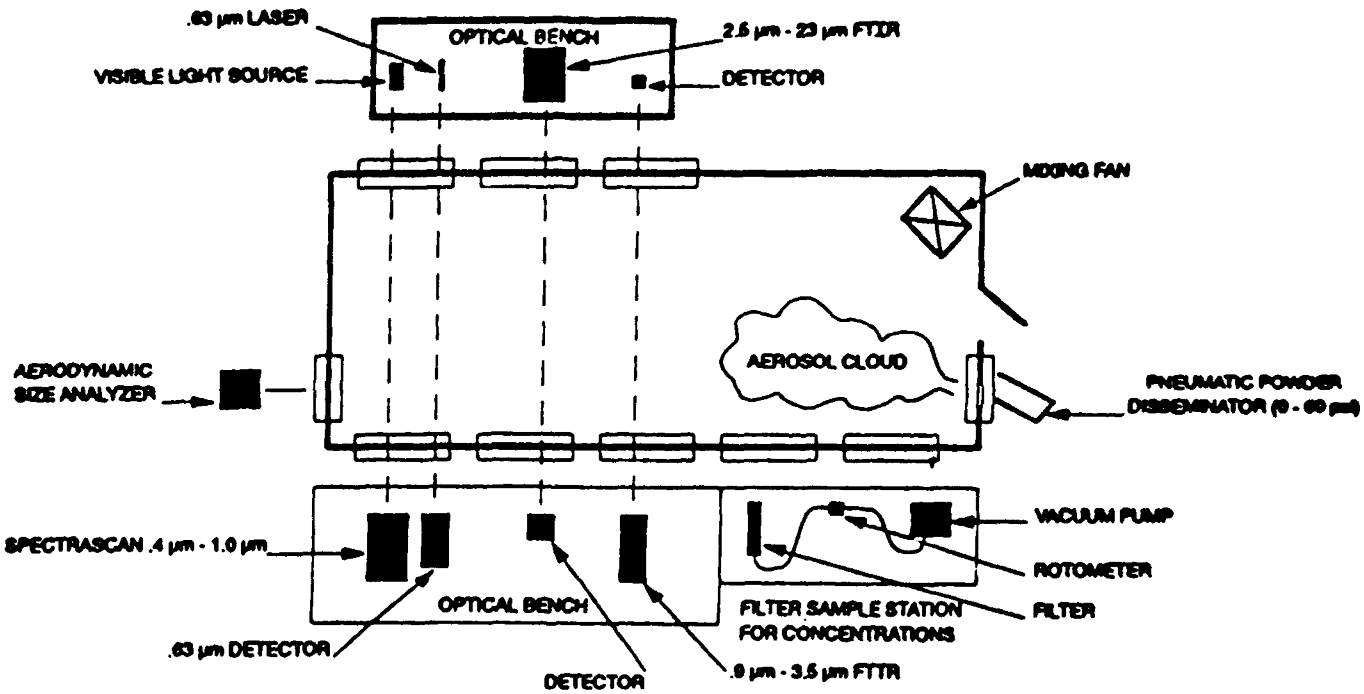

FIGURE 2. 13.6 M^3 AEROSOL CHARACTERIZATION FACILITY

CONCLUSION

The theory of designing a scattering aerosol using a high refractive index material was explained. The concept of describing competing titanium dioxide smoke materials in terms of four measurable performance parameters (extinction coefficient, dissemination yield, deposition velocity and powder packing density) has been presented. Three figures of merit based on these four performance parameters have been introduced. All three are proportional to smoke plume optical depth downwind and can be used not only to rank performance, but also quantitatively to predict cloud opacities downwind or screening areas. The first figure of merit gives the square meters of smoke screening per mass of smoke material transported and is useful in weight limited applications such as the large area smoke generators. The second figure of merit gives the square meters of screening per volume of smoke material transported and is usefull in volume limited applications such as grenades, rockets, artillery rounds, mortars and smoke pots. The third figure of merit gives the square meters of screening per dollar of smoke material cost and is usefull in situations such as training with large area smoke screening. Here for example the weight constraint of the large area smoke generator vehicle would have to be met first by specifying a minimum value for the first figure of merit (weight limited) and then comparing all materials satisfying this constraint based on the third figure of merit (financial limited).

Titanium dioxide manufacturing processes were described and a wide variety of commercially available titanium dioxide powders have been tested in the ERDEC smoke chamber using an SRI sonic pneumatic nozzle at a pressure of 60 psi for dissemination. Performance parameters and their product derived figures of merit are tabulated in Table 1 so that materials can be compared over the visible, 1.06μ, $3\text{-}5\mu$ and $8\text{-}14\mu$ spectral regions. Error analysis of the deposition velocity measurement was presented to explain the large variance. A comparison with deposition rate dominated by Brownian diffusion indicated that gravitational settling and turbulent diffusion/impaction mechanisms are not negligible. Coagulation halflives were computed to demonstrate that significant levels of coagulation occur during chamber testing. Triboelectric charging and electrostatic dispersion of a monopolar charged cloud were discussed to explain the relatively low dissemination yields especially after oven drying.

REFERENCES

1. J.F. Embury, D. Walker, and C.J. Zimmermann, "Screening Smoke Performance of Commercially Available Powders I. Infrared Screening by Graphite Flake", ERDEC TR-93, July 1993

2. E.R. Riley, J.F. Embury and R.H. Frickel, "High Refractive Index Versus High Yield Materials For HC Replacement", Proceedings of the Smoke/Obscurant Symposium XI, AMCPM-SMK-T-001-87, Volume I.

3. N.A. Fuchs, "The Mechanics of Aerosols", Pergamon Press, Macmillam Company, New York(1964).

4. P.C. Reist, Introduction to Aerosol Science, Macmillan Company, New York(1984).

5. Davies, C.N., Aerosol Science, Academic Press, New York(1966).

6. P.A. Lewis, editor, Pigment Handbook, Vol. 1, John Wiley & Sons(1988).

7. Deepak, A., Dissemination Techniques for Aerosols, A. Deepak Publishing, Virginia(1983).

Janon F. Embury and Donald Walker
U.S. Army, Edgewood Research, Development and Engineering Center
Aberdeen Proving Ground, MD 21010-5423

Curtis J. Zimmermann
24 Beale Road
Cold Spring, NY, 10516

PERFORMANCE PARAMETERS AND FIGURES OF MERIT FOR TITANIUM DIOXIDE VISIBLE SCREENING MATERIALS CHAMBER TESTS UTILIZING SRI NOZZLE AT 60 PSI¶

TABLE 1

MATERIAL AND COST§ 10 6 5/4 23/3 10 26	BET SURFACE AREA (m^2/g) PURITY (% TiO_2)	PARTICLE DENSITY $\rho(g_d/cm^3)$	YIELD $Y(g_a/g_d)$	DEPOSITION VELOCITY V_D(cm/sec)	AVG ALPHA $\alpha(m^2/g_a)$ 0.45-0.65μm 1.06μm 3.0-5.0μm 8.0-14.0μm	AVG ALPHA*RHO $\alpha*\rho$ (m^2/cm^3)	WEIGHT LIMITED FIGURE OF MERIT $\Phi_W=\alpha*Y$ (m^2/g_d)	VOLUME LIMITED FIGURE OF MERIT $\Phi_V=\alpha*Y*\rho$ (m^2/cm^3)	FINANCIAL LIMITED FIGURE OF MERIT $\Phi_F=\alpha*Y/COST$ ($m^2/\$$)†
DU PONT R100 @≈ $0.99/lb ≈20 Tons	≈6 ≈97% TiO_2	4.2	0.621	0.088	2.39 2.20 0.22 0.10	10.04 9.24 0.92 0.42	1.48 1.37 0.14 0.06	6.23 5.74 0.57 0.26	676.9 626.6 64.0 27.4
DU PONT R101 @≈ $0.99/lb ≈20 Tons	≈8 ≈97% TiO_2	4.2	0.767	0.051	3.04 2.33 0.16 0.09	12.77 9.79 0.67 0.38	2.33 1.79 0.12 0.07	9.79 7.51 0.52 0.32	1,065.8 818.8 54.9 32.0
DU PONT R102 @≈ $0.99/lb ≈20 Tons	 ≈96% TiO_2	4.1	0.747	0.004	4.45 2.44 0.09 0.14	18.25 10.01 0.37 0.57	3.32 1.82 0.07 0.11	13.63 7.47 0.27 0.43	1,518.7 832.5 32.02 50.3

DU PONT R103 @≈ \$0.99/lb ≈20 Tons	≈12.0 ≈97% TiO_2	4.1	0.597	0.048	3.48 2.25 0.13 0.10	14.27 9.23 0.53 0.41	2.08 1.34 0.08 0.06	8.52 5.51 0.32 0.24	951.5 612.9 36.6 27.4
DU PONT R702 @≈ \$0.99/lb ≈20 Tons	 ≈94% TiO_2	4.0	0.758	0.021	4.04 2.47 0.07 0.11	16.16 9.88 0.28 0.44	3.06 1.87 0.05 0.08	12.25 7.49 0.21 0.33	1,399.7 855.3 22.8 36.6
DU PONT R900 @≈ \$0.99/lb ≈20 Tons	≈12 ≈94% TiO_2	4.0	0.738	0.044	2.87 2.49 0.15 0.10	11.48 9.96 0.60 0.40	2.11 1.84 0.11 0.07	8.47 7.35 0.44 0.29	965.2 841.7 50.3 32.0
DU PONT R901 @≈ \$0.99/lb ≈20 Tons	≈25 ≈85% TiO_2	3.8	0.856	0.032	3.11 2.62 0.16 0.15	11.82 9.96 0.61 0.57	2.66 2.24 0.14 0.13	10.12 8.52 0.52 0.49	1,219.8 1,027.2 73.4 68.8
DU PONT R902 @≈ \$0.99/lb ≈20 Tons	 ≈91% TiO_2	4.0	0.759	0.046	3.10 2.53 0.15 0.12	12.4 10.12 0.60 0.48	2.35 1.92 0.11 0.09	9.41 7.68 0.46 0.36	1,074.9 878.3 50.3 41.2
DU PONT R931 @≈ \$0.99/lb ≈20 Tons	≈40 ≈80% TiO_2	3.6	0.947	0.049	2.69 2.34 0.16 0.12	9.68 8.42 0.58 0.43	2.55 2.22 0.15 0.11	9.18 7.99 0.54 0.40	1,166.4 1,015.5 68.6 50.3
DU PONT R960 @≈ \$1.00/lb ≈20 Tons	 ≈89% TiO_2	3.9	0.640	0.044	2.70 2.55 0.14 0.11	10.53 9.95 0.55 0.43	1.73 1.63 0.09 0.07	6.74 6.36 0.35 0.27	783.5 738.0 40.7 31.7
KEMIRA UNITANE O-110 @≈ \$0.97/lb ≈20 Tons	≈6.6 ≈99% TiO_2	3.9	0.679	0.099	2.52 2.20 0.21 0.13	9.83 8.58 0.82 0.51	1.71 1.49 0.14 0.09	6.67 5.82 0.56 0.34	800.4 697.4 65.5 42.1

KEMIRA UNITANE OR-450 @≈ \$0.97/lb ≈20 Tons	≈9.7 ≈96% TiO_2	4.2	0.598	0.071	3.49 2.40 0.09 0.09	14.66 10.08 0.38 0.38	2.09 1.44 0.05 0.05	8.77 6.03 0.23 0.23	978.2 673.9 23.4 23.4
KEMIRA UNITANE OR-460 @≈ \$0.97/lb ≈20 Tons	≈10.9 ≈97% TiO_2	4.2	0.690	0.020	3.94 2.40 0.09 0.09	16.55 10.08 0.38 0.38	2.72 1.66 0.06 0.06	11.42 6.96 0.26 0.26	1,273.0 776.9 28.1 28.1
KEMIRA UNITANE OR-560 @≈ \$0.97/lb ≈20 Tons	≈22.8 ≈90% TiO_2	4.0	0.692	0.034	3.22 2.61 0.11 0.10	12.88 10.44 0.44 0.40	2.23 1.81 0.08 0.07	8.91 7.22 0.30 0.28	1,043.7 847.2 37.4 32.8
KEMIRA UNITANE OR-572 @≈ \$0.97/lb ≈20 Tons	≈35.3 ≈85% TiO_2	3.9	0.639	0.022	3.32 2.64 0.12 0.14	12.95 10.30 0.47 0.55	2.12 1.69 0.08 0.09	8.27 6.58 0.30 0.35	992.2 791.0 37.4 42.1
KEMIRA UNITANE OR-573 @≈ \$0.97/lb ≈20 Tons	≈30.1 ≈80% TiO_2	3.7	0.851	0.031	3.27 2.44 0.11 0.11	12.10 9.03 0.41 0.41	2.78 2.08 0.09 0.09	10.30 7.68 0.35 0.35	1,301.2 973.5 42.1 42.1
KEMIRA UNITANE OR-580 @≈ \$0.97/lb ≈20 Tons	≈18.5 ≈95% TiO_2	4.1	0.636	0.020	3.75 2.51 0.09 0.10	15.38 10.29 0.37 0.41	2.39 1.60 0.06 0.064	9.78 6.55 0.23 0.26	1,118.6 748.9 28.1 28.1

KEMIRA UNITANE OR-600 @≈ \$0.97/lb ≈20 Tons	≈19.8 ≈95% TiO_2	4.1	0.748	0.025	3.49 2.60 0.11 0.10	14.31 10.66 0.45 0.41	2.61 1.94 0.08 0.07	10.70 7.97 0.34 0.31	1,221.6 908.0 37.4 32.8
KEMIRA UNITANE OR-620 @≈ \$0.97/lb ≈20 Tons	≈20 ≈91% TiO_2	4.1	0.856	0.031	4.04 2.38 0.10 0.11	16.56 9.76 0.41 0.45	3.46 2.04 0.09 0.09	14.18 8.35 0.35 0.39	1,619.4 954.8 42.1 42.1
KERR MCGEE CR-800 @≈ \$0.97/lb ≈10 Tons	≈12.5 ≈95% TiO_2	4.0	0.744	0.024	4.22 2.55 0.08 0.12	16.88 10.20 0.32 0.48	3.14 1.90 0.06 0.09	12.56 7.59 0.23 0.36	1,469.6 889.3 28.1 42.1
KERR MCGEE CR-800 PG @≈ \$0.97/lb ≈10 Tons	≈95% TiO_2	4.1	0.751	0.007	5.08 2.10 0.08 0.14	20.82 8.61 0.33 0.57	3.82 1.58 0.06 0.11	15.64 6.47 0.25 0.43	1,787.9 739.5 28.1 51.5
KERR MCGEE CR-813 @≈ \$0.97/lb ≈10 Tons	≈39.6 ≈86% TiO_2	3.8	0.887	0.048	3.01 2.21 0.18 0.14	11.44 8.40 0.68 0.53	2.67 1.96 0.16 0.12	10.15 7.45 0.61 0.46	1,249.7 917.4 74.9 56.2
KERR MCGEE CR-821 @≈ \$0.97/lb ≈10 Tons	≈92% TiO_2	4.0	0.715	0.041	3.40 2.44 0.11 0.10	13.60 9.76 0.44 0.40	2.43 1.74 0.08 0.07	9.72 6.98 0.31 0.29	1,137.3 814.4 37.4 32.8
KERR MCGEE CR-822 @≈ \$0.97/lb ≈10 Tons	≈90% TiO_2	4.0	0.620	0.035	3.42 2.51 0.11 0.10	13.68 10.04 0.44 0.40	2.12 1.56 0.07 0.06	8.48 6.22 0.27 0.25	992.2 730.1 32.8 28.1
KERR MCGEE CR-828 @≈ \$0.97/lb ≈10 Tons	≈94% TiO_2	4.1	0.922	0.043	3.96 2.55 0.07 0.09	16.24 10.46 0.29 0.37	3.65 2.35 0.06 0.08	14.97 9.64 0.26 0.34	1,708.3 1,099.9 28.1 37.4

KERR MCGEE CR-834 @≈ $0.97/lb ≈10 Tons	≈9.0 ≈97% TiO_2	4.2	0.408	0.066	3.48 2.25 0.12 0.10	14.62 9.45 0.50 0.42	1.42 0.92 0.05 0.04	5.96 3.86 0.21 0.17	664.6 430.6 23.4 18.7
KERR MCGEE CRX NOT COMMERCIAL	≈10.5 ≈97% TiO_2	3.9	0.710	0.036	3.87 2.59 0.07 0.10	15.09 10.10 0.27 0.39	2.75 1.84 0.05 0.07	10.83 7.25 0.20 0.28	NA
KERR MCGEE CR-837 @≈ $0.97/lb ≈10 Tons	≈98% TiO_2	4.0	0.607	0.041	3.69 2.45 0.11 0.10	14.76 9.80 0.44 0.40	2.24 1.49 0.07 0.06	8.96 5.95 0.27 0.24	1,048.4 697.4 32.8 28.1
KRONOS 2020 @≈ $0.99/lb ≈20 Tons	≈12.0 ≈94% TiO_2	4.1	0.903	0.045	3.27 2.59 0.09 0.10	13.41 10.62 0.37 0.41	2.95 2.34 0.09 0.09	12.10 9.60 0.37 0.37	1,349.4 1,070.4 41.2 41.2
KRONOS 2073 @≈ $0.99/lb ≈20 Tons	≈6.8 ≈97% TiO_2	4.2	0.477	0.042	3.41 2.44 0.09 0.10	14.32 10.25 0.38 0.42	1.63 1.16 0.04 0.05	6.83 4.89 0.18 0.20	745.6 530.6 18.3 22.9
KRONOS 2081 @≈ $1.10lb ≈20 Tons	≈12.2 ≈90% TiO_2	4.0	0.444	0.060	3.21 2.38 0.16 0.16	12.84 9.52 0.64 0.64	1.42 1.05 0.07 0.07	5.70 4.23 0.28 0.28	649.6 480.3 32.0 32.0
KRONOS 2085 @≈ $0.99/lb ≈20 Tons	≈90% TiO_2	4.0	0.509	0.040	2.97 2.62 0.11 0.13	11.88 10.48 0.44 0.52	1.51 1.33 0.06 0.07	6.05 5.33 0.22 0.27	690.7 608.3 27.4 32.0
KRONOS 2090 @≈ $0.99/lb ≈20 Tons	≈15.6 ≈94% TiO_2	4.1	0.734	0.044	3.44 2.55 0.10 0.10	14.10 10.46 0.41 0.41	2.52 1.87 0.07 0.07	10.35 7.67 0.30 0.07	1,152.7 855.4 32.0 32.0

KRONOS 2101 @≈ $0.99/lb ≈20 Tons	≈12.0 ≈92% TiO_2	4.0	0.722	0.024	3.01 2.75 0.12 0.10	12.04 11.00 0.48 0.40	2.17 1.99 0.09 0.07	8.69 7.94 0.35 0.29	992.6 910.3 41.2 32.0
KRONOS 2102 @≈ $0.99/lb ≈20 Tons	 ≈94% TiO_2	4.1	0.882	0.018	3.21 2.61 0.10 0.11	13.16 10.70 0.41 0.45	2.83 2.30 0.09 0.10	11.61 9.44 0.36 0.40	1,294.5 1,052.1 41.2 45.7
KRONOS 2131 @≈ $0.99/lb ≈20 Tons	≈63.6 ≈80% TiO_2	3.7	0.908	0.035	2.82 2.56 0.1 0.1	10.43 9.47 0.37 0.37	2.56 2.32 0.09 0.09	9.47 8.60 0.34 0.34	1,171.0 1,061.2 41.2 41.2
KRONOS 2132 @≈ $0.99/lb ≈20 Tons	 ≈80% TiO_2	3.7	0.941	0.034	3.05 2.20 0.16 0.16	11.28 8.14 0.59 0.59	2.87 2.07 0.15 0.15	10.62 7.66 0.56 0.56	1,316.1 949.0 68.8 68.8
KRONOS 2160 @≈ $1.00/lb ≈20 Tons	≈17.4 ≈91% TiO_2	3.9	0.848	0.017	3.24 2.59 0.11 0.11	12 64 10.10 0.43 0.43	2.75 2.20 0.09 0.09	10.72 8.57 0.36 0.36	1,257.9 1,006.3 41.2 41.2
KRONOS 2200 @≈ $0.99/lb ≈20 Tons	≈10.5 ≈96% TiO_2	4.1	0.561	0.040	3.57 2.28 0.08 0.10	14.64 9.35 0.33 0.41	2.00 1.28 0.05 0.06	8.21 5.24 0.18 0.23	914.9 585 5 22.9 27.4
KRONOS 2210 @≈ $0.99/lb ≈20 Tons	≈7.6 ≈96% TiO_2	4.1	0.509	0.045	3.35 2.52 0.09 0.10	13.74 10.33 0.37 0.41	1.71 1.28 0.05 0.05	7.00 5.26 0.19 0.21	782.2 585.5 22.9 22.9
KRONOS 2220 @≈ $0.99/lb ≈20 Tons	≈10.5 ≈93% TiO_2	4.0	0.785	0.026	2.92 2.46 0.13 0.10	11.68 9.84 0.52 0.40	2.29 1.93 0.10 0.08	9.17 7.72 0.41 0.31	1,047.5 882.8 45.7 36.6

KRONOS 2230 @≈ $1.03/lb ≈20 Tons	≈96% TiO_2	4.1	0.928	0.021	4.15 2.44 0.07 0.13	16.60 9.76 0.28 0.52	3.85 2.26 0.07 0.12	15.40 9.06 0.26 0.48	1,761.1 1,033.8 32.0 54.9
KRONOS 2310 @≈ $0.99/lb ≈20 Tons	≈15.0 ≈93% TiC_2	4.0	0.777	0.025	3.14 2.54 0.12 0.10	12.56 10.16 0.48 0.40	2.44 1.97 0.09 0.08	9.76 7.89 0.37 0.31	1,116.1 901.1 41.2 36.3
KRONOS 3020 @≈ $1.05/lb ≈20 Tons	≈2.6 ≈99% TiO_2	4.0	0.118	0.107	1.45 1.65 0.35 0.15	5.80 6.60 1.40 0.60	0.17 0.19 0.04 0.02	0.68 0.78 0.17 0.07	77.8 86.9 18.3 9.1
KRONOS 3025 @≈ $1.05/lb ≈20 Tons	≈2.9 ≈99% TiO_2	4.1	0.513	0.126	1.34 1.51 0.35 0.11	5.49 6.19 1.43 0.45	0.69 0.78 0.18 0.06	2.82 3.18 0.74 0.23	315.6 356.8 82.3 27.4
SCM RCL2 ADHL @≈ $0.99/lb ≈20 Tons	≈18.2 ≈90% TiO_2	4.0	0.711	0.043	2.79 2.61 0.13 0.10	11.16 10.44 0.52 0.4	1.98 1.86 0.09 0.07	7.93 7.42 0.37 0.28	905.7 850.8 41.2 32.0
SCM RCL3 EFNF @≈ $0.99/lb ≈20 Tons	≈50.4 ≈80% TiO_2	3.8	0.982	0.048	2.35 2.14 0.20 0.13	8.93 8.13 0.76 0.49	2.31 2.10 0.20 0.13	8.77 7.99 0.75 0.49	1,056.7 960.6 91.5 59.5
SCM RCL4 ODFGM @≈ $0.99/lb ≈20 Tons	≈97% TiO_2	4.2	0.534	0.049	3.36 2.36 0.11 0.10	14.11 9.91 0.46 0.42	1.79 1.26 0.06 0.05	7.54 5.29 0.25 0.22	818.8 576.4 27.4 22.9
SCM RCL6 GJQW @≈ $0.99/lb ≈20 Tons	≈14.5 ≈88% TiO_2	4.0	0.636	0.030	2.86 2.63 0.13 0.11	11.44 10.52 0.52 0.44	1.82 1.67 0.08 0.07	7.28 6.69 0.33 0.28	832.5 763.9 36.6 32.0

SCM RCL9 6HJTB @≈ \$0.99/lb ≈20 Tons	≈16.3 ≈94% TiO_2	4.1	0.638	0.028	3.28 2.55 0.12 0.10	13.45 10.46 0.49 0.41	2.09 1.63 0.08 0.06	8.58 6.67 0.31 0.26	956.0 745.6 36.6 27.4
SCM R-69 @≈ \$0.99/lb ≈20 Tons	≈6.8 ≈97% TiO_2	4.2	0.726	0.022	4.27 2.46 0.06 0.10	17.93 10.33 0.25 0.42	3.10 1.79 0.04 0.07	13.02 7.50 0.18 0.30	1,418.0 818.8 18.3 32.0
SCM RCL535 @≈ \$0.99/lb ≈20 Tons	≈17.8 ≈95% TiO_2	4.2	0.710	0.035	3.91 2.59 0.09 0.13	16.42 10.88 0.38 0.55	2.92 1.93 0.07 0.10	12.27 8.13 0.28 0.41	1,335.7 882.8 32.0 45.7
SCM RCL628 @≈ \$1.00/lb ≈20 Tons	≈20.0 ≈92%TiO_2	4.0	0.830	0.005	3.97 2.61 0.07 0.13	15.88 10.44 0.28 0.11	3.29 2.17 0.06 0.11	13.18 8.67 0.23 0.43	1,504.9 992.6 27.4 50.3
SCM RGM ANATASE @≈ \$0.96/lb ≈20 Tons	≈15 calculated ≈88% TiO_2	3.9	0.553	0.115	2.74 2.12 0.18 0.13	10.69 8.27 0.70 0.51	1.52 1.17 0.10 0.07	5.91 4.57 0.39 0.28	695.3 535.2 45.7 32.0
SCM RG ANATASE @≈ \$0.96/lb ≈20 Tons	≈15 calculated ≈88% TiO_2	3.9	0.592	0.189	2.11 1.65 0.24 0.13	8.23 6.44 0.94 0.51	1.25 0.98 0.14 0.08	4.87 3.81 0.55 0.30	571.8 448.3 64.0 36.6
TAYCA MT-100F @≈ \$21.00/lb ≈100 lbs	≈60 ≈80% TiO_2	3.9	0.902	0.152	1.36 1.17 0.47 0.10	5.30 4.56 1.83 0.39	1.22 1.06 0.42 0.09	4.78 4.11 1.65 0.35	26.12 22.47 9.03 1.92
TAYCA MT-100T @≈ \$16.00/lb ≈100 lbs	≈60 ≈80% TiO_2	3.9	0.888	0.083	2.32 1.15 0.30 0.10	9.04 4.48 1.17 0.39	2.06 1.02 0.27 0.09	8.03 3.98 1.05 0.35	56.47 27.96 7.40 2.47

TAYCA MT-150W @≈ \$16.00 ≈100 lbs	≈100 ≈90% TiO_2	3.9	0.905	0.132	1.45 1.14 0.44 0.10	5.66 4.45 1.72 0.39	1.31 1.03 0.40 0.09	5.12 4.03 1.56 0.35	35.9 28.2 10.97 2.47
TIOXIDE R-FC2 @≈ \$0.99/lb ≈10 Tons	≈8 ≈97% TiO_2	4.0	0.483	0.065	3.44 2.21 0.13 0.09	13.76 8.84 0.52 0.36	1.66 1.07 0.06 0.04	6.65 4.27 0.25 0.17	759.3 489.4 27.4 18.3
TIOXIDE R-FC6 @≈ \$0.99/lb ≈10 Tons	≈8 ≈97% TiO_2	4.0	0.748	0.001	4.51 2.39 0.09 0.11	18.04 9.56 0.36 0.44	3.37 1.79 0.07 0.08	13.49 7.15 0.27 0.33	1,541.5 818.8 32.0 36.6
TIOXIDE R-HD6X @≈ \$0.99/lb ≈10 Tons	≈13 ≈95% TiO_2	4.0	0.795	0.027	3.89 2.63 0.09 0.13	15.56 10.52 0.36 0.52	3.09 2.09 0.07 0.10	12.37 8.36 0.29 0.41	1,413.5 956.0 32.0 45.7
TIOXIDE R-TC90 @≈ \$0.99/lb ≈10 Tons	≈15 ≈94% TiO_2	4.0	0.709	0.037	3.16 2.44 0.14 0.10	12.64 9.76 0.56 0.40	2.24 1.73 0.10 0.07	8.96 6.92 0.40 0.28	1,024.6 791.4 45.7 32.0
TIOXIDE R-XL @≈ \$0.99/lb ≈10 Tons	≈30 ≈80% TiO_2	3.8	0.779	0.030	3.25 2.53 0.13 0.15	12.35 9.61 0.49 0.57	2.53 1.97 0.10 0.12	9.62 7.49 0.39 0.44	1,157.3 901.1 45.7 54.9
TIOXIDE TR-44 @≈ \$0.99/lb ≈10 Tons	≈9 ≈92% TiO_2	4.0	0.312	0.107	2.82 2.54 0.19 0.17	11.28 10.16 0.76 0.68	0.88 0.79 0.06 0.05	3.52 3.17 0.24 0.21	402.5 361.4 27.4 22.8
TIOXIDE TR-63 @≈ \$1.00/lb ≈10 Tons	≈18 ≈92% TiO_2	4.0	0.662	0.028	3.75 2.65 0.11 0.13	15.00 10.60 0.44 0.52	2.48 1.75 0.07 0.09	9.93 7.01 0.29 0.34	1,134.4 800.5 32.0 41.2

TIOXIDE TR-80 @≈ \$0.99/lb ≈10 Tons	≈13 ≈94% TiO_2	4.0	0.668	0.022	3.82 2.49 0.11 0.12	15.28 9.96 0.44 0.48	2.55 1.66 0.07 0.08	10.20 6.65 0.29 0.32	1,166.4 759.3 32.0 36.6
TIOXIDE TR-92 @≈ \$0.99/lb ≈10 Tons	≈14 ≈94% TiO_2	4.0	0.782	-0.005	4.28 2.72 0.08 0.12	17.12 10.88 0.32 0.48	3.34 2.13 0.06 0.09	13.39 8.51 0.25 0.38	1,527.8 974.3 27.4 41.2
TIOXIDE UF02 @≈ \$10.99/lb ≈1 Tons	≈119 ≈74% TiO_2	3.9	0.958	0.099	2.27 1.30 0.27 0.16	8.85 5.07 1.05 0.62	2.18 1.25 0.26 0.15	8.50 4.88 1.01 0.59	90.1 51.6 10.7 6.2

AVERAGE ALPHA VALUES SELECTED FOR THE FOLLOWING REASONS:

0.45-0.65μm visible light corresponds to the range of maximum photopic and scotopic response for the human eye.

1.06μm is the operating wavelength of neodinium YAG laser designators.

3.0-5.0μm is the operating regime for thermal imaging systems that rely on indium antimonide detectors.

8.0-14.0μm is the operating regime for thermal imaging systems that rely on mercury cadmium telluride detectors.

g_a=grams aerosol, g_d=grams disseminated=grams transported

† (\$/lb)(lb/454g_d)

§ the cost of titanium dioxide presented in this publication is only an approximation based on 1993 prices. It does not represent the actual cost of titanium dioxide which will fluctuate according to a number a factors.

¶ Table 1 is only a measure of performance for different grades of titanium dioxide and should not be considered an endorsement for any particular product or titanium dioxide manufacturer.